# 甘肃龙首山茏岭地区古生代正长岩成因及构造意义

张志强[1)],王凯兴[1,2)],王刚[3)],刘晓东[2,4)],刘文恒[5)],邬斌[2)]

1) 东华理工大学地球科学学院,南昌,330013;
2) 核资源与环境国家重点实验室培育基地,东华理工大学,南昌,330013;
3) 核工业203研究所,陕西咸阳,712000; 4) 九江学院,江西九江,332005;
5) 江西省数字国土重点实验室,东华理工大学,南昌,330013

**内容提要**:甘肃龙首山茏岭正长岩产于茏岭复式岩体中,产有我国少见的交代岩型铀矿床。为揭示正长岩成因,并探讨其构造意义,本文对正长岩进行了岩相学、年代学、地球化学特征等研究。部分斜长石和石英呈椭圆或圆形以包裹体的形式出现在钾长石中、针状磷灰石和角闪石熔蚀现象都暗示茏岭正长岩可能由两种不同性质的岩浆混合形成。锆石LA-ICP-MS U-Pb定年结果显示,茏岭正长岩形成于427.2±3.6 Ma,与北祁连地区同碰撞花岗岩成岩年龄吻合。茏岭正长岩$SiO_2$含量中等,全碱含量为8.49%~11.74%,$K_2O/Na_2O$值为1.07~1.20,属于钾玄岩系列;茏岭正长岩相对富集Rb、Ba、Th、U和Pb,亏损Nb、Ta、P和Ti等元素;稀土元素总量高且相对富集轻稀土,中等Eu亏损;$[n(^{87}Sr)/n(^{86}Sr)]_i$值为0.70798~0.70799,$\varepsilon_{Nd}(t)$值变化于-3.57~-3.35,与区域I型花岗岩类似。综合岩相学、年代学和地球化学特征表明,茏岭正长岩是由壳—幔岩浆混合而成。茏岭正长岩的形成可能与古祁连洋闭合之后,祁连—柴达木板块和阿拉善板块的碰撞有关。由于古祁连洋在奥陶纪晚期(445 Ma)封闭,祁连—柴达木板块与阿拉善板块碰撞,并俯冲到阿拉善板块之下,碰撞引发龙首山断裂右旋走滑形成的局部伸展环境导致软流圈地幔上涌,并加热大陆地壳物质形成长英质岩浆,该长英质岩浆与地幔岩浆混合形成茏岭正长岩。

**关键词**:正长岩;伸展环境;岩浆混合;交代型铀矿床;甘肃龙首山

龙首山成矿带东起甘肃省民勤县红崖山,西至张掖西北,东西长180 km,南北宽几至十余千米。该成矿带已经发现了5个铀矿床、40个矿点、矿化点和两千多个异常点,是一条以碱交代型铀矿化为主要的铀成矿带,铀矿大部分产于钠交代花岗岩内,可归类为钠交代花岗岩型铀矿床(杜乐天,1996,2001;张树明等,2013;陈云杰等,2012,2014;赵如意等,2013,2015;刘金枝,2010)。

茏岭地区位于龙首山铀成矿带中段,区内发育有新水井和茏岭碱交代型铀矿床。茏岭岩体由中细粒闪长岩、花岗闪长岩、中粗粒黑云母花岗岩、正长岩等构成的复式岩体。近些年来关于茏岭地区的研究主要集中于岩石成因和矿床成因等方面的工作,包括茏岭地区花岗岩、花岗闪长岩和闪长岩成因(李占游,1987;陈云杰等,2012,2015;汤琳和张树明,2015;赵亚云等,2015,2016;聂利等,2016;张甲民等,2017),及区内铀矿床成因研究(赵如意等,2013;魏正宇和张玮,2014;陈云杰等,2014;赵如意,2013;刘洪成等,2017;宋振涛等,2017)。然而,对于茏岭地区北部发育的正长岩的研究较为薄弱。巫建华等(2017)研究认为碱交代型铀矿化可能与碱性岩(正长岩或者粗面岩)岩浆作用有关。有鉴于此,本次研究选取茏岭岩体中的正长岩开展了岩相学、年代学、元素和同位素地球化学等工作,旨在探讨其相关的成岩年龄、岩石成因及构造意义,并期望通过本次研究为龙首山茏岭地区碱交代型铀矿床成因的研究提供基础,也为我国西北地区碱交代型铀矿床的寻找与勘探提供进一步的理论依据。

## 1 地质背景

龙首山地区位于华北板块西南缘阿拉善地块的南缘,南临走廊拗陷,北接潮水盆地(图1),是我国

注:本文为国家自然科学基金资助项目(编号:41602071);中国核工业地质局铀矿勘查项目(编号:201619);中国核工业地质局"十三五"高校科研攻关项目的成果。
收稿日期:2017-12-27;改回日期:2018-06-25;责任编辑:章雨旭。Doi:10.16509/j.georeview.2018.04.018
作者简介:张志强,男,1992年生,硕士研究生,地质学专业。Email:1270822341@qq.com。通讯作者:王凯兴,男,1985年生,讲师,硕士生导师,矿产普查与勘探专业。Email:xy2gmo02@ecit.cn。

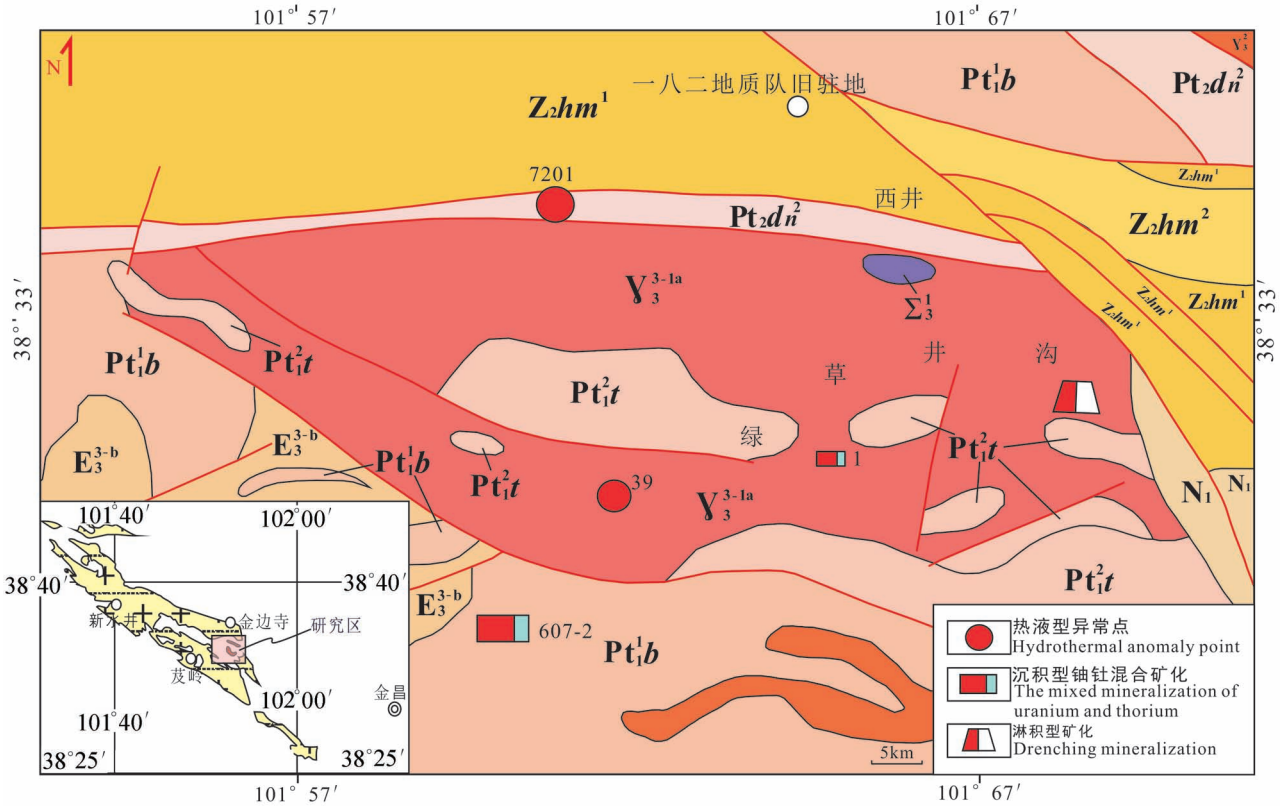


图 1 甘肃龙首山茨岭地区地质简图

Fig. 1 Simplified geological map of the Jiling area in Mt. Longshou, Gansu

$N_1$—新近系;$Zhm^2$—震旦系孩母山群上亚群;$Zhm^1$—震旦系孩母山群下亚群;$Pt_2dn^2$—中元古界墩子沟群下亚群;$Pt_1^2t$—古元古界龙首山群塌马子沟组;$Pt_1^1b$—古元古界龙首山群白家嘴组;$\delta_3^{3-1a}$—加里东晚期一次中粗粒二长花岗岩 $E_3^{3-1b}$—加里东晚期一次碱性杂岩;$\delta_3^1$—加里东早期闪长岩

$N_1$—Neogene; $Zhm^2$—the Upper Subgroup of the Sinian (Ediacaran) Haimushan Group; $Zhm^1$— the Lower Subgroup of Sinian (Ediacaran) Haimushan Group; $Pt_2dn^2$—the Lower Subgroup of the Mesoproterozoic Dunzigou Group; $Pt_1^2t$—the Tamazigou Formation of the Paleoproterozoic Longshoushan Group; $Pt_1^1b$— the Baijiazui Formation of the Paleoproterozoic Longshoushan Group; $\delta_3^{3-1a}$—medium coarse grained adamellite of the first stage of Late Caledonian $E_3^{3-1b}$—alkaline complex of the first stage of Late Caledonian; $\delta_3^1$—Early Caledonian diorites

碱交代型铀矿床代表性地区(陈云杰等,2014)。龙首山—祁连山铀矿成矿带是我国较为重要的铀成矿带,属于古欧亚大陆成矿域中的祁连—秦岭铀成矿省。该成矿域内的铀和其他内生金属矿床均为古生代构造—岩浆活动的产物,矿床成矿年龄主要属于加里东期—海西期,也有部分燕山期的矿化(黄净白等,2005)。区内岩浆活动强烈,岩浆岩出露面积广、种类多,其展布方向与区域构造基本一致。其中加里东晚期岩浆岩最发育,规模较大,系深部陆壳重熔交代成因,产铀的茨岭岩体就是其中之一。区内构造活动强烈,由一系列褶皱、断裂组成。褶皱包括两个不对称的复背斜、复向斜,背斜紧密,向斜开阔。南北缘区域深大断裂和不同方向次级断裂,把整个龙首山切割成若干个菱形、三角形断块。区内铀成矿包括茨岭(701 矿床)和新水井(706 矿床)两个铀矿床及众多个铀矿化点。该区矿化类型较多,有中期混合成因的伟晶白岗岩型(红石泉)、加里东晚期或海西早期的硅质脉型(革命沟),也有淋积型铀矿化(金边寺)、砂岩型、碱性杂岩中的铀矿化等,最具有典型意义的是碱交代型热液铀矿化(赵亚云等,2015)。正长岩位于茨岭岩体中的复式杂岩体中,茨岭岩体是龙首山地区最大的花岗岩类侵入体,也是该地区主要的产铀岩体。岩体长 54 km,宽几千米,面积 174.7 $km^2$,东宽西窄呈楔形侵入于前寒武系龙首山群变质岩中。茨岭复式杂岩体主要由闪长岩、灰白色或肉红色中粗粒花岗岩、细粒花岗岩、花

岗闪长岩正长岩等岩性构成(杜乐天,2001)。南部与变质岩呈侵入接触,北部则为渐变过渡关系。

## 2　岩相学特征

茏岭正长岩位于茏岭复式花岗杂岩体中段,岩石呈肉红色,主要矿物包括石英(5%~10%)、钾长石(71%)、斜长石(14%)、黑云母(2%)、角闪石(4%)。副矿物包括锆石、榍石、磷灰石等。石英粒度 0.01~0.05 $mm^2$,钾长石粒度变化于 0.5×0.1 $mm^2$~1×0.5 mm~2×1.5 $mm^2$,斜长石粒度为 0.8×0.25 $mm^2$~0.5×0.1 $mm^2$,黑云母粒度为 0.8×0.075 $mm^2$,角闪石粒度为 0.3×0.05 $mm^2$。石英具有明显的波状消光和碎裂纹,说明成岩之后可能受到后期应力的影响(图 2a)。斜长石聚片双晶发育,表面有明显的绢云母—水云母化蚀变作用(图 2a)。钾长石主要由正长石、条纹长石和微斜长石构成,以条纹长石为主,表面呈现出明显的泥化现象(图 2a)。少量细小的蠕虫状的石英和斜长石颗粒以包裹体形式出现在钾长石中(图 2b)。黑云母呈现出明显的绿泥石化蚀变,沿着黑云母的解理缝出现大量的暗色不透明铁的氧化物(图 2c);此外,少量黑云母呈现出"云母鱼"的特征,这也佐证了岩体受到了后期应力的影响(图 2d)。角闪石也呈现出绿泥石化蚀变作用,沿着角闪石的解理缝有水云母化现象,大部分角闪石被交代只残留一点轮廓,极少数还保留角闪石原有的晶型(图 2e)。

副矿物包括锆石、榍石、磁铁矿、磷灰石、独居石等。可见大量信封状的榍石,其粒度为 0.05×0.03 $mm^2$~0.1×0.3 $mm^2$。大量针状磷灰石出现在钾长石中(图 2f)。

## 3　分析方法

锆石 U-Pb 年龄测定是在南京大学内生金属矿床成矿机制研究国家重点实验室应用激光剥蚀电感耦合等离子体质谱仪(LA-ICP-MS)完成。ICP-MS 仪器型号为 Agilent7500a,激光剥蚀系统为 New wave UP213 激光器($\lambda$ = 213 nm)。工作参数为:等离子气体(Ar)流量 1.6 L/min,辅助气体(Ar)流量 1 L/min,剥蚀物质载气(He)流量 0.9~1.2 L/min,激光脉冲频率 5Hz,激光束斑直径 30 μm,剥蚀时间

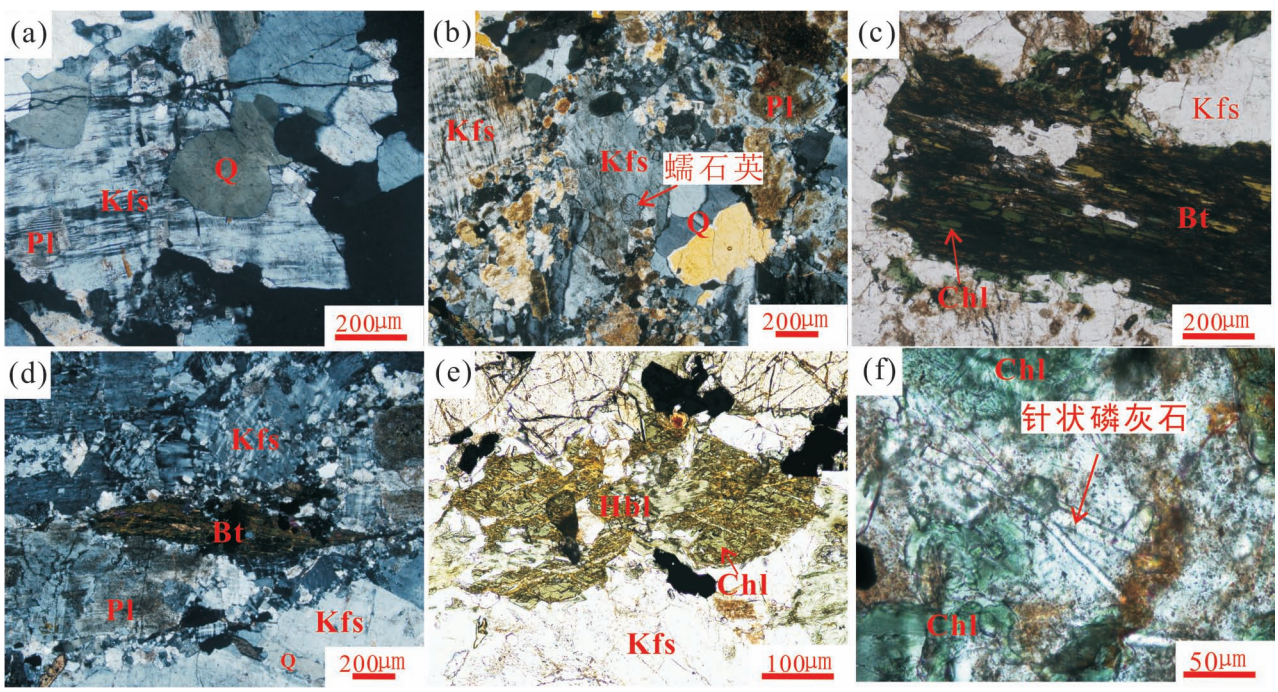


图 2 龙首山茏岭正长岩岩相学显微照片:(a)呈圆形具有波状消光的石英;(b)在钾长石中包裹着一颗蠕石英;(c)黑云母沿解理缝有铁质矿物析出并有绿泥石化作用;(d)受应力作用发生形变的云母,发生绿泥石化蚀变,解理缝有铁质矿物析出;(e)被交代和发生绿泥石化的角闪石;(f)针状磷灰石

Fig. 2 Microphotographs of Jiling syenite in Mt. Longshou: (a) a circular quartz with wavy extinction; (b) a vermicular quartz is wrapped in potash feldspar; (c) the biotite precipitates along the cleavage seam with iron mineral and chloritization; (d) the biotite is deformed by stress with chloritization, along the cleavage seam with iron mineral; (e) amphibolite with metasomatization and chloritization; (f) acicular apatite

90s,背景测量时间 40 s,脉冲能量 10~20 J/cm$^2$,用外标锆石 GEMOC/GJ-1(609 Ma),ICP-MS 的分析数据通过即时分析软件 GLITTER 计算获得同位素比值、年龄和误差,普通铅按照 Andersen 的方法进行校正,校正后的数值应用 Isoplot/Ex Version3.23 完成锆石 U-Pb 年龄谐和图及$^{206}$Pb/$^{238}$U 年龄的加权平均值。

主量、微量元素分析由澳实分析检测集团澳实矿物实验室(广州)完成,主量元素利用荷兰 PANalytical 生产的 Axios 荧光光谱仪(XRF)测试分析。微量元素由美国 Varian 生产的 ICP753-ES 仪器分析,分析方法为岩石样品经四酸消解后,利用电感耦合等离子体发射光谱(ICP-MS)测定多元素含量。稀土元素分析为碱熔法,即将岩石样品加入到 $LiBO_2$熔剂中,混合均匀,在 1000 ℃以上的熔炉中熔化,利用电感耦合等离子体质谱仪检测多种元素含量,检测仪器为美国 Perkin Elmer 公司生产的 Elan9000。

全岩 Sr—Nd—Pb—Hf 同位素化学前处理与质谱测定在南京聚谱检测科技有限公司完成。岩石粉末经高压密闭溶样弹消解后,一部分消解液经过阳离子—锶特效联合树脂,分离出 Sr 和总稀土。总稀土组分再经过 Ln 特效树脂,分离出 Nd。Sr、Nd 淋洗液被蒸干后,先用 1.0 mL 2%稀硝酸溶解,将其作为母液;取其中 50 μL,稀释成 500 μL,在 Agilent 7700x 四极杆型 ICP-MS 上测定 Sr、Nd 准确含量。再用 2%稀硝酸将 Sr、Nd 母液稀释成 $50\times10^{-9}$ Sr、$50\times10^{-9}$ Nd。同位素溶液经 Cetac Aridus II 膜去溶系统引入,在 Nu Plasma II MC-ICP-MS 上测定同位素比值。Sr 同位素比值测定过程中,采用 $n(^{86}Sr)/n(^{88}Sr)=0.1194$ 校正仪器质量分馏。Sr 同位素国际标准物质 NIST SRM 987 作为外标,校正仪器漂移。Nd 同位素比值测定过程中,采用 $n(^{146}Nd)/n(^{144}Nd)=0.7219$ 校正仪器质量分馏。Nd 同位素国际标准物质 JNdi-1 作为外标,校正仪器漂移。

## 4 结果

### 4.1 年代学特征

锆石测年结果见表 1。共选取 19 个锆石进行 LA-ICP-MS 定年,被测锆石无色透明至浅黄褐色,其中未发现明显的矿物包裹体,发育有明显的韵律环带,说明被测锆石为岩浆成因。被测锆石中 Th 的含量为 $671\times10^{-6}$~$4844\times10^{-6}$,U 的含量为 $443\times10^{-6}$~$2547\times10^{-6}$,Th/U 值约 1.5~1.9。点 6 的$^{206}$Pb/$^{238}$U 年龄为 835 Ma,可能为捕获围岩中的锆石;剩余 18 个锆石点的$^{206}$Pb/$^{238}$U 锆石年龄变化在 413~440 Ma 之间,在锆石 U-Pb 年龄谐和图中,18 个数据集中分布在谐和线 420~450 Ma 附近(图 3a)。$^{206}$Pb/$^{238}$U 加权平均年龄为 427.2±3.6 Ma(MSWD=1.5)(图 3b),代表了正长岩的形成年龄,属于加里东期。

### 4.2 地球化学特征

主量元素分析结果见表 2。由表中数据可看出,茏岭正长岩 $SiO_2$ 含量为 59.69%~66.07%,$Al_2O_3$含量为 16.54%~18.02%,CaO 含量为 1.21%~3.68%,MgO 含量为 0.43%~1.32%,$K_2O$ 及 $Na_2O$ 含量分别为 4.39%~6.40%和 4.10%~5.34%,全碱

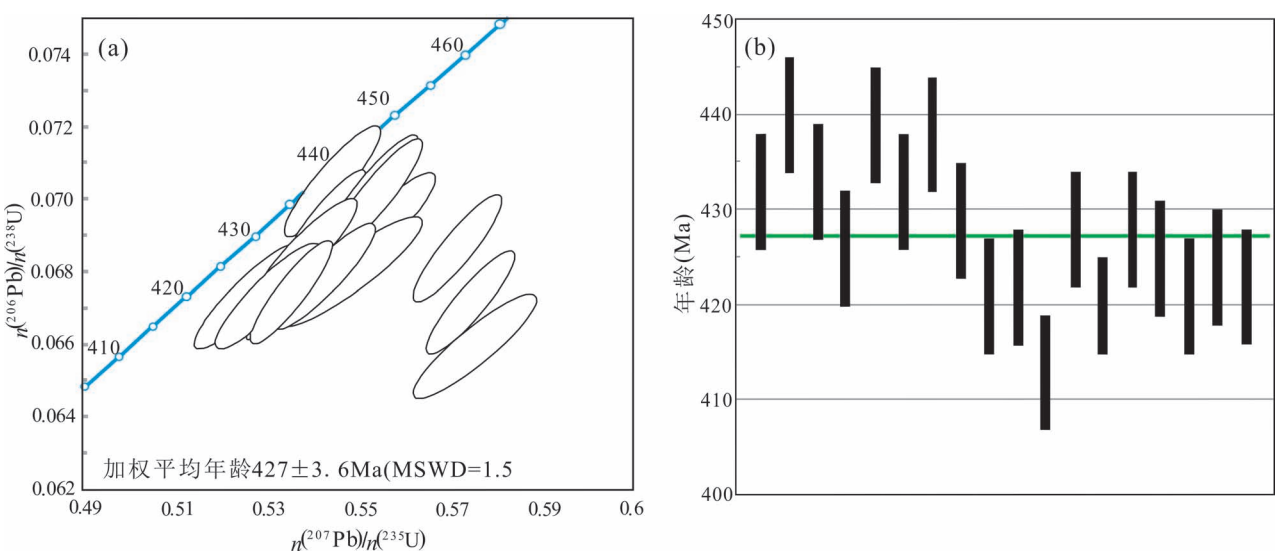


图 3 龙首山茏岭正长岩锆石 U-Pb 年龄谐和图(a)和加权平均年龄图(b)

Fig. 3 Zircon LA-ICP-MS U-Pb concordia diagram of the Jiling syenite in Mt. Longshou

表 1 甘肃龙首山茏岭正长岩 LA-ICP-MS 锆石 U-Pb 同位素分析结果

Table 1 LA-ICP-MS Zircon U-Pb dating data of the Jiling syenite in the Mt. Longshou area, Ganshu

| 测点号 | 元素含量($\times10^{-6}$) | | Th/U | 同位素比值 | | | | | | 同位素年龄(Ma) | | | | | |
|---|---|---|---|---|---|---|---|---|---|---|---|---|---|---|---|
| | Th | U | | $n(^{207}Pb)/n(^{206}Pb)$ | | $n(^{207}Pb)/n(^{235}U)$ | | $n(^{206}Pb)/n(^{238}U)$ | | $n(^{207}Pb)/n(^{206}Pb)$ | | $n(^{207}Pb)/n(^{235}U)$ | | $n(^{206}Pb)/n(^{238}U)$ | |
| | | | | 测值 | 1σ | 测值 | 1σ | 测值 | 1σ | 测值 | 1σ | 测值 | 1σ | 测值 | 1σ |
| ZKG74-1 | 1476 | 1606 | 0.92 | 0.0574 | 0.0007 | 0.5488 | 0.0069 | 0.0694 | 0.0010 | 506 | 14 | 444 | 5 | 432 | 6 |
| ZKG74-2 | 1316 | 1162 | 1.13 | 0.0560 | 0.0007 | 0.5447 | 0.0069 | 0.0706 | 0.0010 | 451 | 14 | 442 | 5 | 440 | 6 |
| ZKG74-3 | 1613 | 1628 | 0.99 | 0.0567 | 0.0006 | 0.5427 | 0.0063 | 0.0695 | 0.0010 | 479 | 14 | 440 | 4 | 433 | 6 |
| ZKG74-4 | 2572 | 2017 | 1.27 | 0.0574 | 0.0006 | 0.5408 | 0.0060 | 0.0684 | 0.0009 | 505 | 14 | 439 | 4 | 426 | 6 |
| ZKG74-5 | 1346 | 1682 | 0.80 | 0.0571 | 0.0006 | 0.5536 | 0.0065 | 0.0704 | 0.0010 | 493 | 14 | 447 | 4 | 439 | 6 |
| ZKG74-6 | 181 | 210 | 0.86 | 0.06812 | 0.00121 | 1.2996 | 0.02265 | 0.13838 | 0.00203 | 872 | 16 | 846 | 10 | 835 | 11 |
| ZKG74-7 | 2853 | 985 | 2.90 | 0.0581 | 0.0008 | 0.5556 | 0.0076 | 0.0694 | 0.0010 | 533 | 14 | 449 | 5 | 432 | 6 |
| ZKG74-8 | 2060 | 1844 | 1.12 | 0.0572 | 0.0006 | 0.5546 | 0.0064 | 0.0703 | 0.0010 | 501 | 14 | 448 | 4 | 438 | 6 |
| ZKG74-9 | 2600 | 985 | 2.64 | 0.0697 | 0.0009 | 0.6693 | 0.0084 | 0.0697 | 0.0010 | 920 | 13 | 520 | 5 | 434 | 6 |
| ZKG74-10 | 3226 | 2547 | 1.27 | 0.0603 | 0.0006 | 0.5718 | 0.0063 | 0.0688 | 0.0010 | 613 | 14 | 459 | 4 | 429 | 6 |
| ZKG74-11 | 886 | 664 | 1.33 | 0.0566 | 0.0008 | 0.5267 | 0.0076 | 0.0675 | 0.0009 | 475 | 14 | 430 | 5 | 421 | 6 |
| ZKG74-12 | 1042 | 1777 | 0.59 | 0.0574 | 0.0007 | 0.5355 | 0.0063 | 0.0677 | 0.0009 | 505 | 13 | 435 | 4 | 422 | 6 |
| ZKG74-13 | 948 | 639 | 1.48 | 0.0631 | 0.0010 | 0.5757 | 0.0087 | 0.0662 | 0.0009 | 711 | 14 | 462 | 6 | 413 | 6 |
| ZKG74-14 | 1813 | 1613 | 1.12 | 0.0569 | 0.0007 | 0.5383 | 0.0063 | 0.0686 | 0.0009 | 488 | 13 | 437 | 4 | 428 | 6 |
| ZKG74-15 | 1368 | 2004 | 0.68 | 0.0619 | 0.0007 | 0.5747 | 0.0063 | 0.0674 | 0.0009 | 670 | 13 | 461 | 4 | 420 | 5 |
| ZKG74-16 | 671 | 813 | 0.83 | 0.0569 | 0.0008 | 0.5388 | 0.0074 | 0.0687 | 0.0010 | 488 | 14 | 438 | 5 | 428 | 6 |
| ZKG74-17 | 1233 | 443 | 2.79 | 0.0584 | 0.0011 | 0.5488 | 0.0103 | 0.0682 | 0.0010 | 544 | 19 | 444 | 7 | 425 | 6 |
| ZKG74-18 | 1040 | 762 | 1.36 | 0.0570 | 0.0008 | 0.5308 | 0.0074 | 0.0675 | 0.0009 | 492 | 14 | 432 | 5 | 421 | 6 |
| ZKG74-19 | 2797 | 960 | 2.91 | 0.0579 | 0.0008 | 0.5432 | 0.0072 | 0.0681 | 0.0009 | 525 | 14 | 440 | 5 | 424 | 6 |

($Na_2O + K_2O$)含量为 8.49%～11.74%，$K_2O/Na_2O$ 值 1.07～1.20，$Mg^{\#}$为 23～26。在 TAS 图中(图 4a)，样品落入 Irvine 分界线以上，即正长岩区域。在 $SiO_2$—$K_2O$图解中(图 4b)，样品位于钾玄岩系列；样品的 A.R 值为 2.73～4.09，在 A.R—$SiO_2$图中(图 4c)，样品落入碱性系列区域；A/CNK 为 0.89～0.99，在 A/CNK—A/NK 图解中(图 4d)，样品落入准铝质范畴。综上，茏岭地区正长岩属于准铝质—碱性—正长岩系列。

茏岭地区正长岩类微量元素及稀土元素分析结果见表 2。在原始地幔标准化蛛网图上(图 6a)，所有样品均显示出相对富集 Rb、Ba、Th、U 和 Pb 等大离子亲石元素(LILE)，相对亏损 Nb、Ta、P 和 Ti 等高场强元素。其中以 Nb 和 Ta 的负异常较为显著。利用微量元素对茏岭正长岩进行花岗岩类型判别(图 5)，10000 • Ga/Al—Nb(图 5a)和 10000 • Ga/Al—(Zr + Ce + Nb + Y)(图 5b)，所有样品点均落在 A-型花岗岩之中，表明茏岭正长岩为 A-型花岗岩。

岩体富含稀土元素，总稀土含量为 $158.80\times10^{-6}$～$590.49\times10^{-6}$(均值 $445.12\times10^{-6}$)，ΣLREE为 $150.88\times10^{-6}$～$568.57\times10^{-6}$(均值 $426.38\times10^{-6}$)，ΣHREE为 $7.92\times10^{-6}$～$25.47\times10^{-6}$(均值 $18.75\times10^{-6}$)，LREE/HREE 为 19.05～25.94(均值 22.43)，$(La/Yb)_N$ 为 25.02～40.14(均值 33.42)。在稀土元素球粒陨石标准化配分图中(图 6b)，样品为左倾轻稀土富集型，

表 2 甘肃龙首山茏岭正长岩主量元素(%)、微量元素($\times10^{-6}$)和稀土元素($\times10^{-6}$)分析结果

Table 2 Major elements (%), Trace elements($\times10^{-6}$) and rear earth elements ($\times10^{-6}$) analysis results of the Jiling syenite in the Mt. Longshou area, Ganshu

| | ZKG74-1-1 | ZKG74-1-3 | ZKG74-1-4 | ZK-1 | ZK-2 | | ZKG74-1-1 | ZKG74-1-3 | ZKG74-1-4 | ZK-1 | ZK-2 |
|---|---|---|---|---|---|---|---|---|---|---|---|
| $SiO_2$ | 61.87 | 66.07 | 59.69 | 65.41 | 62.06 | La | 179 | 131 | 143 | 110 | 139 |
| $TiO_2$ | 0.53 | 0.46 | 0.7 | 0.4 | 0.55 | Ce | 279 | 216 | 265 | 184 | 254 |
| $Al_2O_3$ | 17.81 | 16.54 | 18.02 | 16.86 | 17.71 | Pr | 24.9 | 19.8 | 25.9 | 16.4 | 23.4 |
| $TFe_2O_3$ | 3.38 | 2.83 | 4.19 | 2.66 | 3.48 | Nd | 74.1 | 60.3 | 82.5 | 50.5 | 74.1 |
| CaO | 1.68 | 1.21 | 3.68 | 2.11 | 2.36 | Sm | 10.3 | 8.65 | 12 | 7.11 | 10.4 |
| $K_2O$ | 6.4 | 5.69 | 5.33 | 5.07 | 5.86 | Eu | 1.82 | 1.54 | 2.33 | 1.43 | 2.04 |
| $Na_2O$ | 5.34 | 5.09 | 4.72 | 4.97 | 4.81 | Gd | 6.86 | 6 | 8.37 | 5.25 | 7.29 |
| MgO | 0.89 | 0.76 | 1.32 | 0.71 | 0.93 | Tb | 0.98 | 0.82 | 1.12 | 0.73 | 1.05 |
| MnO | 0.07 | 0.06 | 0.1 | 0.05 | 0.07 | Dy | 5.58 | 4.79 | 6.5 | 4 | 5.53 |
| $P_2O_5$ | 0.17 | 0.14 | 0.27 | 0.16 | 0.21 | Ho | 1.12 | 0.9 | 1.29 | 0.81 | 1.13 |
| 烧失 | 1.71 | 1.18 | 1.93 | 1.55 | 1.22 | Er | 3.24 | 2.68 | 3.66 | 2.25 | 3.23 |
| Co | 4.2 | 3.5 | 6.1 | 3.4 | 4.7 | Tm | 0.49 | 0.4 | 0.54 | 0.36 | 0.5 |
| Cr | 3 | 2 | 3 | 3 | 3 | Yb | 3.19 | 2.67 | 3.47 | 2.3 | 3.26 |
| Cs | 1.78 | 3.24 | 3.09 | 3.4 | 3.3 | Lu | 0.46 | 0.4 | 0.52 | 0.37 | 0.46 |
| Ni | 2 | 2.5 | 2.5 | 2.4 | 3 | Hf | 11.6 | 9.8 | 11.8 | 8.7 | 11.1 |
| Pb | 61.3 | 63.8 | 59 | 51.8 | 64.5 | Nb | 35.7 | 32.3 | 37.5 | 29.7 | 35.8 |
| V | 35 | 30 | 57 | 27 | 42 | Ta | 2.8 | 2.5 | 3.1 | 2.3 | 2.8 |
| Zn | 51 | 43 | 64 | 39 | 56 | Th | 159 | 117 | 107 | 83.2 | 116 |
| Ga | 18.7 | 17.9 | 20.9 | 20.7 | 20.7 | U | 15.2 | 15.8 | 12.3 | 7.53 | 10.3 |
| Ba | 1445 | 1240 | 1595 | 1255 | 1830 | Y | 27.4 | 25 | 29 | 20.5 | 29.1 |
| Rb | 146 | 151 | 135 | 164 | 160 | Zr | 549 | 432 | 583 | 352 | 506 |
| Sr | 513 | 455 | 915 | 569 | 806 | | | | | | |

δCe 为 0.90~1.00(均值 0.95),δEu 为 0.62~0.72(均值 0.67),为中等程度的 Eu 负异常。

茏岭正长岩同位素分析结果见表 3,其 $[n(^{87}Sr)/n(^{86}Sr)]_i$ 值为 0.70798~0.70799,$\varepsilon_{Nd}(t)$ 值变化于-3.57~-3.35。

## 5 讨论

### 5.1 岩石成因

目前,关于正长岩的成因,主要由以下几种认识:

(1)由于幔源岩浆和挥发份物质注入到下地壳底部导致下地壳岩石的部分熔融(Lubala et al., 1994),或者封闭系统中地壳岩石在加厚的大陆地壳压力下部分熔融(Huang Wenlai and Wyllie, 1981)。

(2)可能是和俯冲相关的交代地幔部分熔融(Sutcliffe et al., 1990; Lynch et al., 1993)或者碱性玄武质岩浆分离结晶的产物(Parker, 1983; Brown and Becker, 1986; Thorpe and Tindle, 1992; Yang Jinhui et al., 2005; Rios et al., 2007)。

(3)可能是岩浆混合,特别是幔源基性岩浆和酸性岩浆混合后分异的产物(Barker et al., 1975; Sheppard, 1995; Zhao Jianxin et al., 1995; Litvinovsky et al., 2002)或者幔源硅不饱和碱性岩浆和下地壳部分熔融形成的花岗质岩浆混合的产物(Dorais, 1990)。

笔者等认为,茏岭地区正长岩可能是由于岩浆混合所致。下面将从岩相学、元素地球化学和同位素地球化学等方面对这一认识进行论证。

茏岭正长岩的岩相学特征暗示岩浆混合作用。

表 3 甘肃龙首山茏岭正长岩 Rb-Sr 和 Sm-Nd 同位素分析结果

Table 3 Rb-Sr and Sm-Nd isotopic compositions of the Jiling syenite in the Mt. Longshou area, Ganshu

| 样品号 | $\frac{n(^{87}Sr)}{n(^{86}Sr)}$ | $\frac{n(^{87}Rb)}{n(^{86}Sr)}$ | $\left[\frac{n(^{87}Sr)}{n(^{86}Sr)}\right]_i$ | $\frac{n(^{143}Nd)}{n(^{144}Nd)}$ | $\frac{n(^{147}Sm)}{n(^{144}Nd)}$ | $\left[\frac{n(^{143}Nd)}{n(^{144}Nd)}\right]_t$ (CHUR) | $\varepsilon_{Nd}(t)$ | $T_{DM}$ (Ga) | $T_{DM2}$ (Ga) |
|---|---|---|---|---|---|---|---|---|---|
| ZK-1 | 0.713215 | 0.83 | 0.70799 | 0.512136 | 0.0859 | 0.512071 | -3.57 | 1.21 | 1.47 |
| ZK74-1 | 0.713138 | 0.82 | 0.70798 | 0.512142 | 0.0841 | 0.512071 | -3.35 | 1.19 | 1.45 |

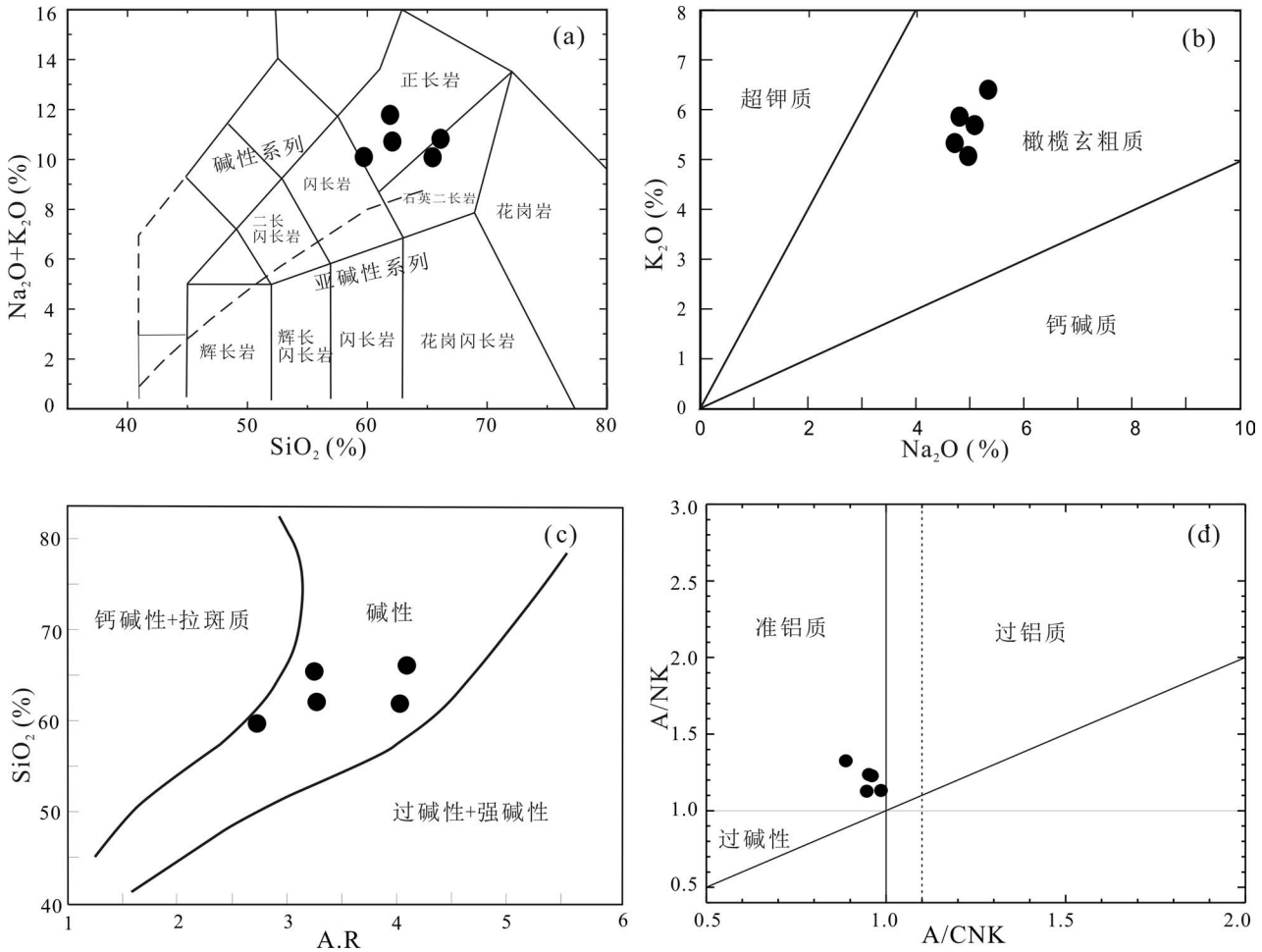


图 4 龙首山茨岭地区正长岩 TAS 图(a)(底图据 Middlemost, 1994)、$K_2O$ —$Na_2O$ 图(b)(底图据 Turner et al., 1996)、A.R—$SiO_2$图(c)(底图据 Wright, 1969)和 A/CNK—A/NK 图(d)(底图据 Maniar and Piccoli, 1989)

Fig. 4 TAS (a), $K_2O$ —$Na_2O$ (b), A.R—$SiO_2$(c) and A/CNK—A/NK (d) diagrams for the Jiling syenite in Mt. Longshou (after Middlemost,1994; Turner et al., 1996; Wright, 1969; Maniar and Piccoli, 1989;respectively)

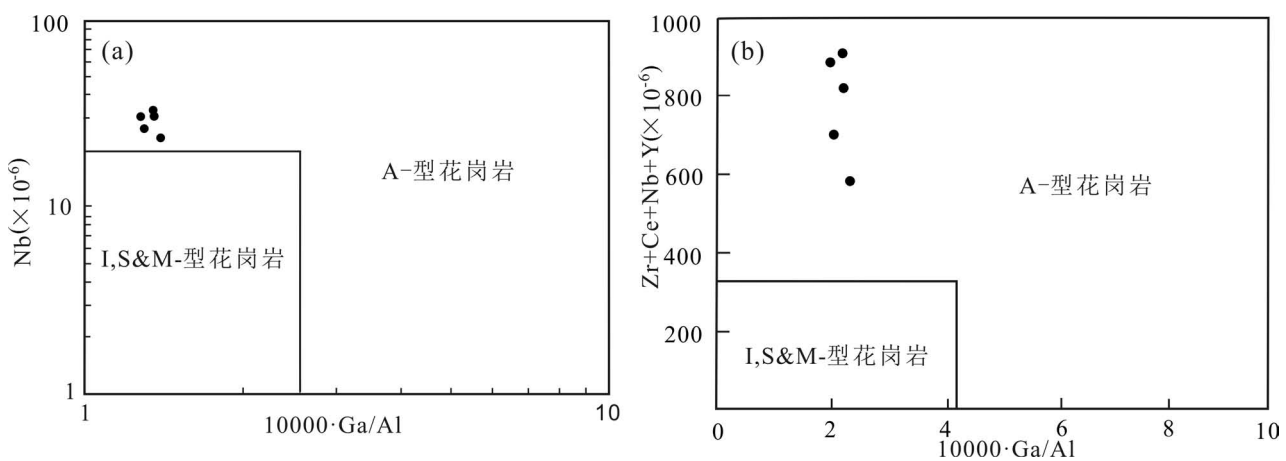


图 5 龙首山茨岭正长岩 A 型花岗岩判别图解(据 Whalen et al.,1987)

Fig. 5 A-type granite discriminant diagrams for the Jiling syenite in the Mt. Longshou (after Whalen et al.,1987)

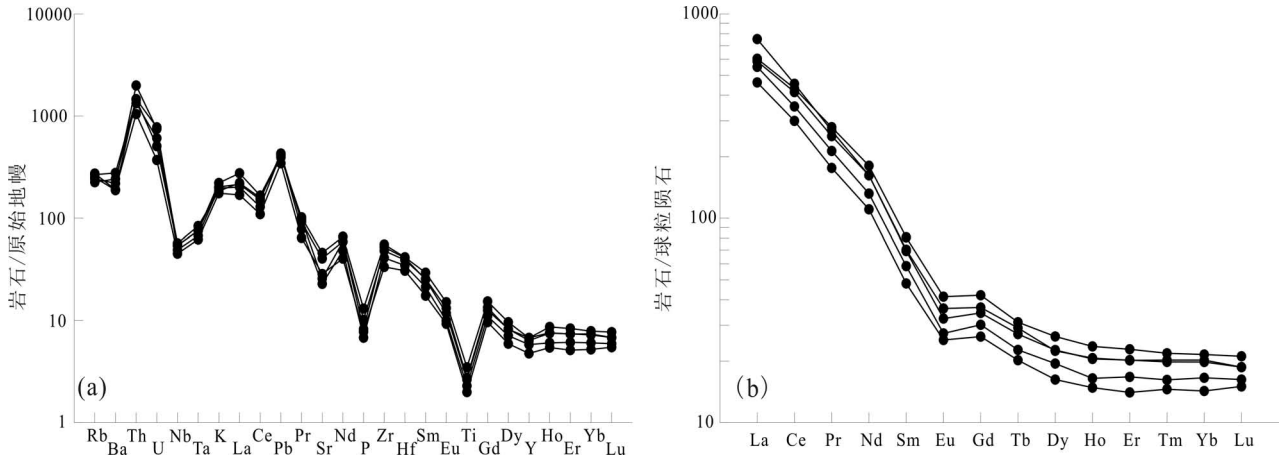


图 6 龙首山茏岭正长岩微量元素原始地幔标准化蛛网图(a,标准化值据 Sun and McDonough, 1989)和稀土元素球粒陨石标准化分布型式图(b,标准化值据 Boynton, 1984)

Fig. 6 Primitive-mantle-normalized trace element spidergrams (a, primitive-mantle data are from Sun and McDough, 1989) and chondrite-normalized REE patterns (b, chondrite data are from Boynton, 1984) of the Jiling syenite in the Mt. Longshou

少量多孔角闪石的形成可能与早期在花岗质岩浆中形成的角闪石被后期混入的高温铁镁质岩浆加热熔融有关(图 2e);大量针状磷灰石的出现为岩浆快速冷却的产物,它的形成可能与高温铁镁质岩浆遇到低温长英质岩浆时快速冷却有关(图 2f)。

茏岭正长岩元素地球化学特征也说明它们可能是由岩浆混合形成。首先,在在 $FeO^T$—MgO 图解中(图 7a),茏岭正长岩与岩浆混合趋势线一致;其次,由于岩浆混合过程中相容元素和不相容元素会呈现出截然不同的特征(Langmuir et al., 1978),可以通过相容元素和不相容元素构成的图解去重塑岩浆作用过程(Schiano et al., 2010)。在图 1/V—Rb/V 关系图上(图 7b),茏岭正长岩与岩浆混合的趋势吻合,说明它们可能是壳幔岩浆混合的产物;最后,岩体中 $SiO_2$ 与其他主要元素呈一定的线性关系,一般可以归因于岩浆分离结晶或两种不同熔体的混合(Lee and Bachmann, 2014)。然而,P 在玄武质岩浆结晶分异过程中可能表现为扭曲的特征(图 8)。在玄武质岩浆体系下,P 随着 $SiO_2$ 的增加而逐步富集,并结晶出磷灰石,当 P 以矿物形式出后,在岩浆中 P 的含量减少(Lee and Bachmann, 2014; Chen Ming et al., 2016)。茏岭的 $SiO_2$ 和 $P_2O_5$ 呈近直线的负线性关系(图 8),说明茏岭正长岩为岩浆混合成因。

Sr—Nd 同位素也从侧面说明茏岭正长岩的形成于岩浆混合有关。在 $[n(^{87}Sr)/n(^{86}Sr)]_i$—$\varepsilon_{Nd}(t)$ 图,茏岭正长岩样品均落入古生代 I 型花岗

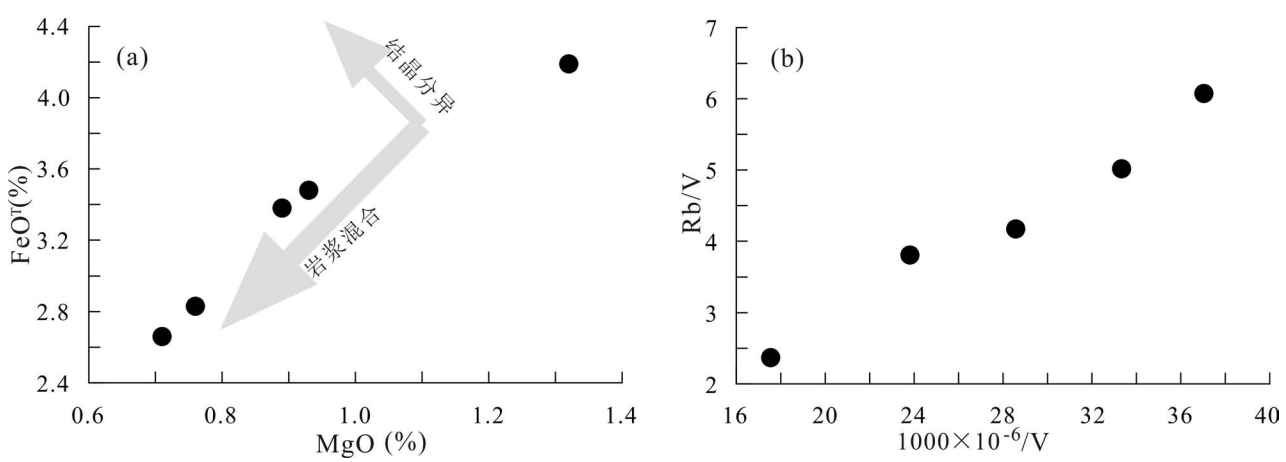


图 7 龙首山茏岭正长岩 MgO—$FeO^T$ 图(a)和 1/V—Rb/V 图(b)

Fig. 7 MgO—$FeO^T$ (a) and 1/V—Rb/V (b) diagrams for the Jiling syenite in the Mt. Longshou

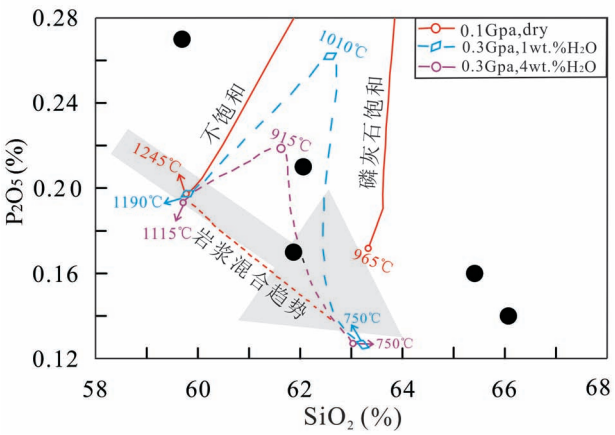


图 8 龙首山茏岭正长岩 $SiO_2$—$P_2O_5$图
（据 Lee and Bachmann，2014）

Fig. 8 $SiO_2$—$P_2O_5$ diagram for the Jiling syenite in the Mt. Longshou (after Lee and Bachmann, 2014)

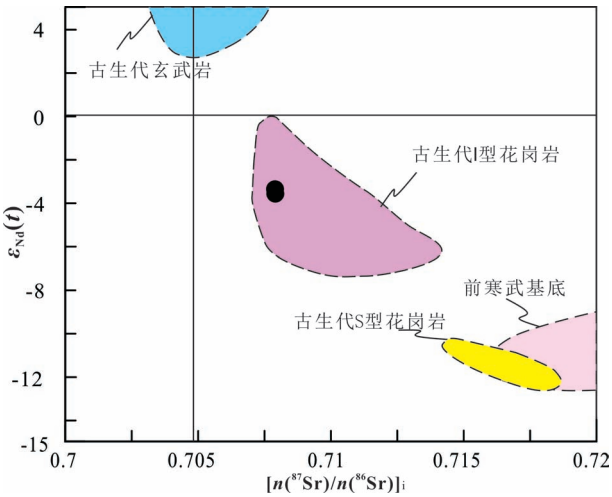


图 9 甘肃龙首山茏岭正长岩$[n(^{87}Sr)/n(^{86}Sr)]_i$—$\varepsilon_{Nd}(t)$图（据 Zhang Liqi et al.，2017）

Fig. 9 $n(^{87}Sr)/n(^{86}Sr)]_i$—$\varepsilon_{Nd}(t)$ diagram for the Jiling syenite in the Mt. Longshou (Zhang Liqi et al., 2017)

岩区域（图 9）与北祁连山 I 型花岗岩类似。I 型花岗岩形成机理有两种，分别为铁镁质岩浆部分熔融与壳幔岩浆混合。结合岩相学、元素地球化学特征，笔者等认为茏岭正长岩为岩浆混合形成。

### 5.2　构造意义

近年来，随着对祁连山地区研究的深入，该区的蛇绿岩套主要可以分为两带：南带和北带。南带蛇绿岩形成于 520~497 Ma，代表了俯冲环境；北带蛇绿岩形成于 490~448 Ma，代表了弧后环境，至晚奥陶世（445 Ma），古祁连洋彻底闭合，北祁连山地区进入板内演化阶段（Song Shuguang et al.，2013）。北祁连山地区花岗岩的形成年龄和构造意义同样也体现了上述特征。按照花岗岩的成岩年龄和特征，北祁连山地区的花岗岩也可以分为三类：与洋壳俯冲有关的火山弧花岗岩，形成于 520~460 Ma 之间（吴才来等，2010；Xia Xiaohong and Song Shuguang，2010；Xia Xiaohong et al.，2012；Song Shuguang et al.，2013；Chen Yixiang et al.，2015）；形成于洋壳封闭后与碰撞有关的花岗岩年龄为 460~420 Ma（Yu Shengyao et al.，2015）；后碰撞花岗岩，形成年龄小于 420 Ma（Song Shuguang et al.，2013；Zeng Renyu et al.，2016）。上述岩石组合和特征记录了古生代北

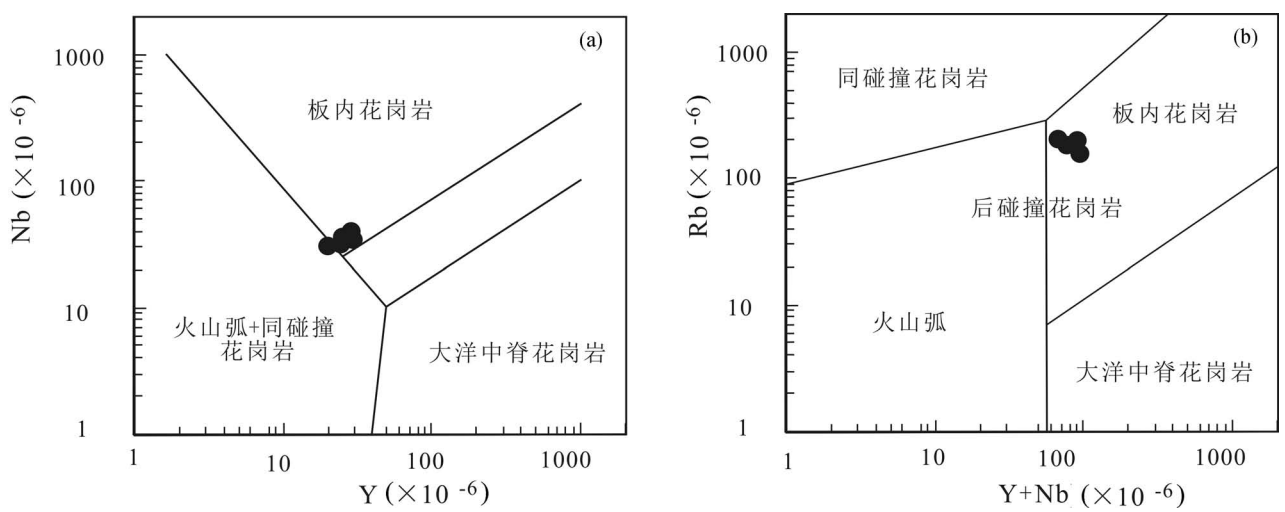


图 10 甘肃龙首山茏岭地区正长岩 Y—Nb（a）和 Y+Nb—Rb（b）图（据 Pearce et al.，1994）

Fig. 10 The Y—Nb (a) and Y+Nb—Rb (b) diagrams of the Jiling syenite in the Mt. Longshou (after Pearce et al., 1994)

祁连山地区由洋壳俯冲闭合到陆陆碰撞,再到板内伸展等这一大地构造演化史。

自古祁连洋闭合后,北祁连山地区发育的岩浆岩根据其岩石地球化学特征可以划分为两类。第一类为成岩年龄介于 467~440 Ma 的低 Mg 高锶低钇中酸性岩(adakite),这些高锶低钇中酸性岩被认为是起源于挤压环境下加厚大陆下地壳部分熔融的产物(Tseng et al., 2009; Yu Shengyao et al., 2015, 2017; Zhang Liqi et al., 2017);第二类主要形成于 440 Ma 之后的高 Mg 高锶低钇中酸性岩、A-型和 I-型花岗岩以及基性岩,这些岩石一般归类为起源于伸展环境下岩浆作用的产物(Zhang Liqi et al., 2017; Zeng Renyu et al., 2016; Tseng et al., 2009; Yu Shengyao et al., 2015, 2017)。

茨岭地区正长岩的成岩年龄为 427.2±3.6 Ma,与北祁连山地区第二类花岗岩成岩年龄吻合,说明茨岭正长岩可能形成于伸展环境。在前人的研究中一些正长岩通常和碱性长英质岩石,以及碱性镁铁质岩石伴生,构成连续的演化系列,碱性岩浆岩通常被认为形成于伸展构造背景下(Whalen et al., 1987; Sylvester, 1989; Eby, 1990, 1992; Barbarin, 1999),因此,这些正长岩也可能形成于伸展背景下(Litvimovsky et al., 2002)这与前人对于正长岩研究结果类似。研究表明,正长岩主要被认为主要形成于伸展环境,包括大洋岛弧、大陆弧、碰撞后和板内伸展环境。Y—Nb 图和(Y+Nb)—Rb 图中(图 10a 和 b),茨岭正长岩落入板内环境区域。因此,笔者等认为茨岭正长岩的形成可能与古生代时期祁连洋闭合后祁连—柴达木板块和阿拉善板块碰撞—俯冲时导致龙首山断裂右旋走滑作用形成的板内伸展环境有关。

## 6 结论

(1)龙首山茨岭地区正长岩形成锆石 LA-ICP-MS 年龄为 427.2±3.6 Ma,为中志留世岩浆作用的产物。

(2)茨岭地区正长岩具有中等程度 $SiO_2$ 含量、准铝质,富集高场强元素,亏损大离子亲石元素元素,属于 A-型花岗岩;岩石稀土元素总量高,轻稀土元素相对富集,Eu 负异常中等;它们的 Sr—Nd 同位素与北祁连山 I 型花岗岩类似。岩相学、元素和同位素地球化学特征指示茨岭地区正长岩的形成可能与岩浆混合有关。

(3)茨岭地区正长岩的形成可能与北祁连洋闭合后祁连—柴达木板块向阿拉善板块的碰撞—俯冲有关。碰撞—俯冲引发龙首山深大断裂右旋走滑产生局部相对伸展环境,地幔岩浆上涌加热中下地壳物质形成长英质岩浆,并与之混合,形成茨岭地区正长岩。

## 参 考 文 献 / References

(The literature whose publishing year followed by a "&" is in Chinese with English abstract; The literature whose publishing year followed by a "#" is in Chinese without English abstract)

陈云杰,赵如意,武彬.2012. 甘肃龙首山地区茨岭铀矿床隐爆角砾岩发现及成因探讨. 地质与勘探,48(6):1101~1108.

陈云杰,傅成铭,王刚,赵如意.2014. 花岗岩型热液铀矿床 C、O 同位素研究——以甘肃省龙首山茨岭矿区为例. 地质与勘探,50(4):641~648.

陈云杰,赵如意,聂利,王刚.2015. 甘肃龙首山地区茨岭岩体锆石 U-Pb 年龄及地质意义. 地质论评, 61(z1):616~617.

杜乐天.1996. 中国铀矿地质研究成果荟萃.《铀矿地质》编辑部.

杜乐天.2001. 中国热液铀矿基本成矿规律和一般热液成矿学. 北京:原子能出版社.

黄净白,黄世杰. 2005. 中国铀资源区域成矿特征. 铀矿地质,21(3):129~138.

李占游.1987. 西北某花岗岩型碱交代热液铀矿床稀土元素地球化学. 铀矿地质,(3):49~57.

刘洪成,宋振涛,叶发旺.2017. 龙首山茨岭岩体南带铀成矿地质条件及找矿方向. 矿产与地质,31(4):657~665.

聂利,赵如意,陈旭,冯博,王刚,李莹.2016. 甘肃省龙首山成矿带茨岭岩体闪长岩特征及其与铀成矿关系. 现代地质,30(4):760~769.

宋振涛,祁程,张伟,赵立信,陈云杰,王生云.2017. 革命沟矿床蚀变分带及元素地球化学特征. 地质论评,63(增刊):173~174.

汤琳,张树明.2015. 龙首山茨岭复式岩体岩石地球化学特征及构造环境探讨.东华理工大学学报,38(3): 265~272.

吴才来,徐学义,高前明,李向民,雷敏,郜源红,Frost B F, Wooden J L. 2010. 北祁连早古生代花岗质岩浆作用及构造演化. 岩石学报,26(4): 1027~1044.

魏正宇,张玮.2014. 甘肃茨岭铀矿床围岩蚀变特征及其与铀矿化的关系. 地质学刊,38(1):150~153.

巫建华,郭国林,郭佳磊,张旗,吴仁贵,余达淦.2017. 中国东部中生代岩浆岩的时空分布及其与热液铀矿的关系. 岩石学报,33(5):1591~1614

张甲民,赵如意,王刚,聂利.2017. 甘肃茨岭似斑状花岗岩地质特征及其地质意义. 地质论评,63(增刊):89~90.

张树明,魏正宇,张良,汤琳,赵新胤.2013. 龙首山碱交代型铀矿床特征和存在的问题. 矿物学报,(增刊 2):284~285.

赵如意,陈云杰,武彬,王刚.2013. 甘肃龙首山茨岭地区钠交代型铀矿成矿模式研究. 地质与勘探,49(1):67~74.

赵如意,姜常义,陈旭,王刚,陈云杰,聂利.2015. 甘肃省龙首山成矿带中段钠长岩脉地质特征及其与铀矿化关系研究. 地质与勘探,51(6):1069~1078.

赵亚云, 张树明, 汤琳, 尧宏福. 2015. 龙首山中断加里东期花岗岩浆作用与铀成矿作用研究述评. 甘肃地质,24(2):71~78.

赵亚云,张树明,汤琳,尧洪福,杨春四.2016. 龙首山中段茨岭花岗岩体 Sr—Nd—Pb 同位素特征及意义. 地质科学,41(6):1016~1030.

Barbarin B.1999. A review of the relationships between granitoid types, their origins and their geodynamic environments. Lithos,46(3):605~626.

Barker F,Wones D R,Sharp W N and Desborough G A.1975. The Pikes Peak batholith,Colorado front range,and a model for the origin of the gabbro—anorthosite—syenite—potassic granite suite. Precambrian Research,2(2):97~160.

Boynton W V.1984. Cosmochemistry of the Rare Earth Elements . In: Henderson P (ed.). Rare Earth Element Geochemistry, Developments in Geochemistry,3~114.

Brown P E and Becker S M.1986. Fractionation, hybridisation and magma-mixing in the Kialineq centre East Greenland.Contributionsto Mineralogy and Petrology,92(1):57~70.

Chen Ming,Sun Min,Cai Keda,Buslov Mikhail M,Zhao Guochun,Jiang Yingde,Rubanova Eiena S,Kulikova Anna V,Voytishek Elena E. 2016. The early Paleozoic tectonic evolution of the Russian Altai: Implications from geochemical and detrital zircon U - Pb and Hf isotopic studies of meta-sedimentary complexes in the Charysh - Terekta - Ulagan - Sayan suture zone. Gondwana Research,34:1~15.

Chen Yixiang, Gao Peng, Zheng Yongfei.2015. The anatectic effect on the zircon Hf isotope composition of migmatites and associated granites. Lithos, 238:174~184.

Chen Yunjie, Fu Chengming, Wang Gang, Zhao Ruyi.2014&.Study on C and O isotopes of granite-type hydrothermal uranium deposits: a case study of the Jiling syenite in the Mt. Longshou area, Gansu. Geology and Exploration, 50 (4):641~648.

Chen Yunjie, Fu Chenming, Wang Gang, Zhao Ruyi, Wang Wei, Miao Huajun. 2014&. Carbon and Oxygen isotopes in Granite-type hydrothermal uranium deposits: a case of the Jiling Uranium Ore Fields in Longshou Mountain, Gansu Province. Geology and Exploration, 50(4):641~648.

Chen Yunjie, Zhao Ruyi, Nie Li, Wang Gang.2015&.Zircon U-Pb age and geological significance of the Jiling rock mass in the Mt. Longshou area, Gansu. Geological Review, 61 (S1):616~617.

Chen Yunjie, Zhao Ruyi, Wu Bin. 2012&. Discover and genesis of cryptoexplosive breccia for the Jiling syenite in the Mt. Longshou area, Gansu. Geology and Exploration, 48 (6):1101~1108.

Dorais M J.1990. Compositional variations in pyroxenes and amphibolesf the Belknap Mountain complex, New Hampshire: Evidence for the origin of silica-saturated alkaline rocks.American Mineralogist,75(9~10):1092~1105.

Du Letian. 2001 #. Basic Metallogenic Regularities and General Hydrothermal Mineralization of Hydrothermal Uranium Deposits in China. Beijing: Atomic Energy Press.

Eby G N.1990. The A-type granitoids: A review of their occurrence and chemical characteristics and speculations on their petrogenesis. Lithos,26(1~2):115~134.

Eby G N. 1992. Chemical subdivision of the A-type granitoids: Petrogenetic and tectonic implications. Geology,20(7):641~644.

Huang Jingbai, Huang Shijie. 2005&. Regional metallogenic characteristics of China's Uranium resources. Uranium Geology, 21 (3):129~138.

Huang Wenlai and Wyllie P J.1981. Phase relationships of S-type granite with $H_2O$ to 35kbar: Muscovite granite from Harney Peak, SouthDakota. Journal of Geophysical Research,86 (NB11):10515~10529.

Langmuir C H,Hanson G N,Hart S R. 1978. A general mixing equation with applications to Icelandic basalts. Earth and Planetary Science Letters,37(3): 380~392.

Lee Cin-Ty A, Bachmann O. 2014. How important is the role of crystal fractionation in making intermediate magmas? Insights from Zr and P systematics. Earth and Planetary Science Letters, 393:266 - 274.

Li Zhanyou.1987#. Rare earth element geochemistry of a granite-type alkali-intercalated hydrothermal uranium deposit in Northwest China. Uranium Geology, (3):49~57.

Litvinovsky B A, Jahn B M, Zanvilevich A N, Saunders A, Poulain S, Kuzmin D V, Reichow M K, Titov A V.2002b. Petrogenesis of syenite - granite suites from the Bryansky Complex (Transbaikalia, Russia): implications for the origin of A-type granitoid magmas. Chemical Geology, 189:105~133.

Litvinovsky B A, Jahn B, Zanvilevich A N and Shadaev M G.2002a. Crystal fractionation in the petrogenesis of an alkali monzodiorite—syenite series: The Oshurkovo plutonic sheeted complex, Transbaikalia,Russia. Lithos,64(3~4):97~130.

Liu Hongcheng, Song Zhentao, Ye Fawang. 2017&. Uranium metallogenic geological conditions and prospecting direction in the southern belt of the Jiling rock mass in the Mt. Longshou. Mineral Resources and Geology, 31 (4):657~665.

Lubala R T, Frick C, Rogers J H, Walraven F.1994. Petrogenesis of syenites and granites of the Schiel alkaline complex, northern Transvaal, South Africa. The Journal of Geology, 102 (3):307~316.

Lynch D J,Musselman T E,Gutmann J T, Patchett P J. 1993. Isotopic evidence for the origin of Cenozoic volcanic rocks in the Pinacate volcanic field, northwestern Mexico. Lithos, 29(3~4):295~302.

Maniar P D, Piccoli P M.1989. Tectonic discrimination of granitoids. Geological Society of America Bulletin, 101(5):635~643.

Middlemost E A K.1994. Naming materials in the magma igneous rock system. Earth-Science Review, 37:215~224.

Nie Li, Zhao Ruyi, Chen Xu, Feng Bo, Wang Gang, Li Yin.2016&. Characteristics of diorite from the Jiling Formation in the Mt. Longshou area metallogenic belt, Gansu Province and their relationship with uranium mineralization. Modern Geology, 30 (4): 760~769.

Parker D F.1983. Origin of the trachyte—quartz trachyte—peralkalic rhyolite suite of the Oligocene Paisano volcano,Trans-Pecos Texas. Geological Society of America Bulletin,94(5):614~629.

Pearce J A, Harris N B W, Tindle A G. 1984. Trace element discrimination diagrams for the tectonic interpretation of granitic rocks. Journal of Petrology, 25:956~983.

Rios D C,Conceicao H,Davis D W,Cid J P,Rosa M L S,Macambira M J B,Mc Reath I,Marinho M M and Davis W J.2007. Paleoproterozoic potassic—ultrapotassic magmatism:Morro do Afonso Syenite Pluton, Bahia,Brazil. Precambrian Research,15(1~2):1~30.

Schiano P, Monzier M, Eissen J P, Martin H, Koga K T.2010. Simple mixing as the major control of the evolution of volcanic suites in the Ecuadorian Andes. Contributions to Mineralogy and Petrology, 160: 297~312.

Sheppard S.1995. Hybridization of shoshonitic lamprophyre and calc-alkaline granite magma in the Early Proterozoic Mt. Bundey igneoussuite, Northern Territory. Australian Journal of Earth Sciences: An International Geoscience Journal of the Geological Society of Australia,42(2):173~185.

Song Shuguang, Niu Yaoling, Su Li, Xia Xiaohong.2013. Tectonics of the North Qilian orogen, NW China. Gondwana Research, 23(4):

1378~1401.

Song Zhentao, Qi Cheng, Zhang Wei, Zhao Lixin, Chen Yunjie, Wang Shengyun. 2017&. Alteration zone and elemental geochemical characteristics of the Geminggou deposit. Geological Review, 63 (S1):173~174.

Sun S S, McDonough W F. 1989. Chemical and isotopic systematics of oceanic basalts: Implications for mantle composition and processes. In:Saunders A D and Norry M J. eds. Magmatism in Oceanic Basins. Geological Society, London, Special Publications, 42(1):313~345.

Sutcliffe R H, Smith A R, Doherty W and Barnett R L. 1990. Mantlederivation of Archean amphibole-bearing granitoid and associate mafic rocks:Evidence from the southern Superior province, Canada. Contributions to Mineralogy and Petrology, 105(3):255~274.

Sylvester P J.1989. Post-collisional alkaline granites. Journal of Geology, 9(3):261~280.

Tang Lin, Zhang Shuming. 2015&. Geochemical characteristics of Jiling Compositie Pluton in Longshou Mountain and Tectonic Environment discussion. Journal of East China Institute of Technology, 38(3): 265~272.

Thorpe R S and Tindle A G.1992. Petrology and petrogenesis of a tertiary bimodal dolerite—peralkaline/subalkaline trachyte/rhyolite dykeassociation from Lundy, Bristol Channel, UK. Geological Journal,27(2):101~117.

Tseng Chienyuan, Yang Huan-Jen, Yang Houngyi, Liu Dunyi, Wu Cailai, Cheng Chiukuang, Chen Chenghong, Ker Choomuar. 2009. Continuity of the North Qilian and North Qinling orogenic belts, Central Orogenic System of China: Evidence from newly discovered Paleozoic adakitic rocks. Gondwana Research, 16:285~293.

Turner S, Arnaud N, Liu K, Rogers N, Hawkesworth C, Harris N, Kelley S, Van Calsterren P, Deng W. 1996. Postcollision, shoshonitic volcanism on the Tibetan, plateau: implications for convective thinning of the lithosphere and source of ocean island basalts. Journal of Petrology, 37:45~71.

Wei Zhengyu, Zhang Wei.2014&.Characteristics of wall rock alteration and its relationship with uranium mineralization in the Jiling uranium deposit, Gansu. Jiangsu Geology, 38 (1):150~153.

Whalen J B,Currie K L,Chappell B W.1987. A-type ganites:geochemical characteristics, discrimination and petrogenesis. Contrib Mineral Petrol.95:407~419.

Wright J B.1969. A simple alkalinity ratio and its application to questions of nonorogenic granite genesis. Geological Magazine, 370~384.

Wu Cailai, Xu Xueyi, Gao Qianming, Li Xiangmin, Lei Min, Gao Yuanhong, Frost B F, Wooden J L. 2010&. Early Paleozoic granitoid magmatism and tectonic evolution in North Qilian, NW China. Acta Petrologica Sinica, 26(4):1027~1044.

Wu Jianhua, Guo Guolin, Guo Jialei, Zhang Qi, Wu Rengui, Yu Dagan. 2017&. Temporal and spatial distribution of Mesozoic Magmatic Rocks in eastern China and their relationship with hydrothermal uranium deposits. Acta Petrologica Sinica, 33 (5): 1591~1614.

Xia Xiaohong, Song Shuguang, Niu Yaoling. 2012. Tholeiite—boninite terrane in the North Qilian suture zone:Implications for subduction initiation and back-arc basin development. Chemical Geology, 328 (11):259~277.

Xia Xiaohong, Song Shuguang. 2010. Foming age and tectono-petrogenises of the Jiuequan ophiolite in the North Qilian Mountain, NW China. Chinese Science Bulletin, 55(18):1899~1907.

Yang Jinhui, Chung Sunlin, Wilde Simon, Wu Fuyuan, Chu Meifei, Lo Chinghua, Fan Hongrui.2005. Petrogenesis of post-orogenic syenites in the Sulu Orogenic Belt, East China: geochronological, geochemical and Nd – Sr isotopic evidence. Chemical Geology, 214:99~125.

Yu Shengyao, Zhang Jianxin, Qin Haipeng, Sun Deyou, Zhao Xilin, Cong Feng, Li Yunshuai.2015. Petrogenesis of the early Paleozoic low-Mg and high-Mg adakitic rocks in the North Qilian orogenic belt, NW China:Implications for transition from crustal thickening to extension thinning. Journal of Asian Earth Sciences, 107:122~139.

Yu Shengyao, Zhang Jianxin, Li Sanzhong, Sun Deyou , Peng Yinbiao, Zhao Xiin. 2017. Continuity of the North Qilian and North Altun orogenic belts of NW China: evidence from newly discovered Palaeozoic low-Mg and high-Mg adakitic rocks. Geological Magazine:1~21.

Zeng Renyu, Lai Jianqing, Mao Xiancheng, Li Bin, Ju Peijiao, Tao Shilong. 2016. Geochemistry, zircon U-Pb dating and Hf isotopies composition of Paleozoic granitoids in Jinchuan, NW China: Constraints on their petrogenesis, source characteristics and tectonic implication. Journal of Asian Earth Sciences 121:20~33.

Zhang Jiamin, Zhao Ruyi, Wang Gang, Nie Li. 2017&. Geological characteristics and geological significance of the porphyry granite of the Jiling, Gansu. Geological Review, 63 (S1):89~90.

Zhang Liqi,Zhang Hongfei,Zhang Shasha,Xiong Ziliang, Luo Biji, Yang He, Pan Fabin, Zhou Xiaochun, Xu Wangchun, Guo Liang.2017. Lithospheric delamination in post-collisional setting: Evidence from intrusive magmatism from the North Qilian orogen to southern margin of the Alxa block, NW China. Lithos,288~289:20~34.

Zhang Shuming, Wei Zhenyu, Zhang Liang, Tang Lin, Zhao Xinyin. 2013&. Characteristics and existing problems of the Mt. Longshou alkali metasomatic uranium deposit. Acta Mineralogica Sinica, (S2):284~285.

Zhao Jianxin,Shiraishi K,Ellis D J and Sheraton J W.1995. Geochemical andisotopic studies of syenites from the Yamato Mountains, East Antarctica: Implications for the origin of syenitic magmas. Geochimica et Cosmochimica Acta,59(7):1363~1382.

Zhao Ruyi, Chen Yunjie, Wu Bin, Wang Gang. 2013&. Study on metallogenic model of sodium metasomatous uranium deposit in the Jiling syenite in the Mt. Longshou area, Gansu. Geology and Exploration, 49 (1):67~74.

Zhao Ruyi, Jiang Changyi, Chen Xu, Wang Gang, Chen Yunjie, Nie Li. 2015&. Geological characteristics of the albitite dyke in the middle segment of the Mt. Longshou metallogenic belt, Gansu Province and their relationship with uranium mineralization. Geology and Exploration, 51 (6):1069~1078.

Zhao Yayun, Zhang Shuming, Tang Lin, Yao Hongfu, Yang Chunsi. 2016&.Sr—Nd—Pb isotopic characteristics and significance of the Jiling granite in the middle section of the Mt. Longshou. Geological Science, 41 (6):1016~1030.

Zhao Yayun, Zhang shuming, Tang Lin, Yao Hongfu. 2015&. Caledonian granitic magmatism and U mineralization in middle Longshoushan. Gansu Geology, 24(2):71~78.

# Petrogenesis and Tectonic Significances of the Paleozoic Jiling Syenite in the Mountain Longshou Area, Gansu Province

ZHANG Zhiqiang[1)], WANG Kaixing[1,2)], WANG Gang[3)], LIU Xiaodong[2,4)], LIU Wenheng[5)], WU Bin[2)]

1) *School of Earth Sciences, East China University of Technology, Nanchang*, 330013;

2) *State Key Laboratory Breeding Base of Nuclear Resources and Environment, Nanchang*, 330013;

3) *The No.* 203 *Institute of Nuclear Industry, Xianyang, Shaaxi*, 712000;

4) *Jiujiang University, Jiujiang, Jiangxi*, 332005;

5) *Key Laboratory of Jiangxi Digital Land, School of Earth Sciences, Nanchang*, 330013

**Objectives**: Jiling syenites occur in the Jiling batholith, developing metasomatite-related uranium deposit which is rarely presented in China. To explore, the genesis and tectonic significant, petrographic, geochronologic, and geochemical analyses were conducted on the Jiling syenites.

**Methods**: Field investigation, syenite sampling and observation under a microscope were performed to obtain lithology, LA-ICP-MS zircon U-Pb dating, analysis of geochemical characteristics of major, trace and rear earth elements, isotopic geochemical analysis were used.

**Result**: Both plagioclase and quartz grains as ellipse or round-shape in the K-feldspar, acicular apatite and porous amphibole indicate that the Jiling syenites may be formed by magma mixing. LA-ICP-MS zircon U-Pb dating reveals the Jiling syenites emplaced at 427±3.6Ma, which is consistent with those of collision-related granitoids in northern Qilian Mountains area. The Jiling syenites show intermediate $SiO_2$ contents, total alkaline contents ranging from 8.49% to 11.74% with $K_2O/Na_2O$ from 1.07 to 1.20, can be classified as shoshonitic type. In the Jiling syenites, Rb, Ba, Th, U and Pb are enriched, while Nb, Ta, P and Ti are depleted; REE contents are high with moderate negative Eu anomalies; the initial Sr isotopic compositions display ranging from 0.70798 to 070799, and $\varepsilon_{Nd}(t)$ from −3.57 to −3.35, which fall in the I-type granitoids area of northern Qilian Mountains area. Combined with petrographic, geochronologic, and geochemical characteristics, writers consider that the Jiling syenites were formed by mixing of crustal-derived and mantle-derived magmas.

**Conclusions**: The formation of the Jiling syenites may have relationship with collision between the Alax and Qilian—Qaidam Blocks. Due to the closure of the Paleo-Qilian Ocean at 445 Ma, the Qilian—Qaidam Block collided with the Alax Block, and subducted underneath the Alax Block. It would lead right-lateral strike-slip of the Mountain Longshou fault, and generate in an extensional environment. The continental crust heated by the upwelling of asthenosphere, and generate the felsic magmas. Mixing of the felsic magma and the mantle-derived magma formed the Jiling syenites.

**Keywords**: syenite; extensional environment; magma mixing; metasomatism-type uranium deposit; Mountain Longshou, Gansu

**Acknowledgements**: This paper is project of *the National Natural Science Foundation of China* (No. 41602071); the uranium exploration project of *China Nuclear Industry Geological Bureau* (No. 201619) and the achievements of the "13rd-five" scientific research project of *the University of China Nuclear Industry Geological.*

**First author**: ZHANG Zhiqiang, male, born in 1992 , master graduate student of geology major. Email: 1270822341@qq.com

**Corresponding author**: Corresponding author: WANG Kaixing, male , born in 1985, lecturer, master student supervisor of mineral survey and exploration major. Email: xy2gmo02@ecit.cn

Manuscript received on: 2017-12-27; Accepted on: 2018-06-25; Edited by: ZHANG Yuxu

**Doi**: 10.16509/j.georeview.2018.04.018